MODIS observation of aerosols and estimation of aerosol radiative forcing over southern Africa during SAFARI 2000

Charles Ichoku,[1,2] Lorraine A. Remer,[2] Yoram J. Kaufman,[2] Robert Levy,[1,2] D. Allen Chu,[1,2] Didier Tanré,[3] and Brent N. Holben[4]

Received 23 March 2002; revised 25 October 2002; accepted 2 January 2003; published 12 April 2003.

[1] MODIS provides almost complete global coverage daily. Aerosol optical thickness (AOT or $\tau_{a\lambda}$) and other aerosol parameters are retrieved over land and ocean at a spatial scale of 10 km (level 2), then aggregated to a global grid of 1° spatial resolution on daily, weekly, and monthly time scales (level 3). The SAFARI 2000 ground-based measurements of AOT from the Aerosol Robotic Network (AERONET) group of Sun photometers were used to compare MODIS over-land AOT based on a spatiotemporal statistical technique. At low aerosol loading (when $\tau_{a470} < 0.6$), MODIS $\tau_{a\lambda}$ values agree with those of AERONET at the blue wavelength (λ = 440, 470 nm). But, at higher wavelengths and with increasing aerosol loading, MODIS AOT values underestimate those of AERONET. There are also regional variations in validation accuracy. This AOT underestimation by MODIS during SAFARI 2000 is attributed to the application of a constant single-scattering-albedo (SSA or ω_0) value of 0.90 globally for smoke aerosol retrieval. Recent studies based on long-term observations with AERONET Sun photometers suggest that lower ω_0 values of 0.88 and 0.84 at 440 nm and 670 nm wavelengths respectively would be more applicable over southern Africa (particularly over Zambia, where most of the measurements were based). A column climate model, with MODIS aerosol information as input, is used to calculate aerosol radiative forcing over the (southern Atlantic) Ocean part of the SAFARI 2000 region. For September 2000, the results show a forcing of -10 W/m^2 at the top of the atmosphere and approximately -26 W/m^2 at the terrestrial surface. *INDEX TERMS:* 0305 Atmospheric Composition and Structure: Aerosols and particles (0345, 4801); 1610 Global Change: Atmosphere (0315, 0325); 1640 Global Change: Remote sensing; 3359 Meteorology and Atmospheric Dynamics: Radiative processes; *KEYWORDS:* MODIS, aerosol, radiative forcing, atmosphere, SAFARI, southern Africa

Citation: Ichoku, C., L. A. Remer, Y. J. Kaufman, R. Levy, D. A. Chu, D. Tanré, and B. N. Holben, MODIS observation of aerosols and estimation of aerosol radiative forcing over southern Africa during SAFARI 2000, *J. Geophys. Res.*, *108*(D13), 8499, doi:10.1029/2002JD002366, 2003.

1. Introduction

[2] Aerosol parameters are among the level 2 products generated operationally from the radiance data acquired by the Moderate resolution Imaging Spectroradiometer (MODIS) sensor. MODIS was launched on 18 December 1999 aboard the Earth Observing System (EOS) Terra satellite, which flies in a near-polar orbit, with daylight equator crossing times of around 10:30 am. MODIS covers the earth almost completely daily. It has 36 spectral channels spread along the 0.405–14.385 μm range of the electromagnetic spectrum. MODIS radiance data exist in three spatial resolutions: 250 m (two channels), 500 m (five channels), and 1 km (29 channels). Numerous parameters describing the physical characteristics of the oceans, land, and the atmosphere are derived from MODIS data as level 2 and higher level products http://modis.gsfc.nasa.gov/data/index.html). Aerosol parameters are retrieved with different approaches over land and ocean, because of the difference in the reflective properties of land and ocean surfaces [*Kaufman et al.*, 1997a; *Tanre et al.*, 1997]. The main aerosol parameter retrieved from MODIS is the aerosol optical thickness (AOT or $\tau_{a\lambda}$). Over land, AOT is retrieved at 470 nm and 660 nm wavelengths (then interpolated at 550 nm), while over ocean it is retrieved at 550, 660, 870, 1200, 1600, and 2100 nm (then extrapolated to 470 nm). Other essential parameters retrieved include Ångstrom exponent over both land and ocean, and effective radius and the fractional contribution of the small size mode to AOT over ocean only. All these are level 2 aerosol products derived at 10-km spatial resolution. MODIS level 3 aerosol

[1]Science Systems and Applications, Inc., Lanham, Maryland, USA.
[2]Laboratory for Atmospheres, NASA/GSFC, Greenbelt, Maryland, USA.
[3]Laboratoire d'Optique Atmosphérique, Centre National de la Recherche Scientifique et Université des Sciences et Technologies de Lille, Villeneuve d'Ascq, France.
[4]Laboratory for Terrestrial Physics, NASA/GSFC, Greenbelt, Maryland, USA.

0148-0227/03/2002JD002366$09.00

products are generated by aggregating the level 2 products onto a global grid at 1° spatial resolution on a daily, 8-day (weekly), and monthly basis.

[3] Comprehensive strategies and procedures have been developed for validating the aerosol products (especially the level 2) around the world [*Chu et al.*, 2002; *Ichoku et al.*, 2002; *Remer et al.*, 2002b]. The validations are performed from the global, regional, and local perspectives, using mainly ground-based measurements from the Aerosol Robotic Network (AERONET) Sun photometers [*Holben et al.*, 1998, 2001]. The results showed that prelaunch accuracy estimates were achieved [*Chu et al.*, 2002; *Remer et al.*, 2002b]. In particular, validation was conducted separately for certain distinct aerosol source regions around the world. For the southern African region, *Chu et al.* [2002] compared MODIS and AERONET aerosol measurements representing the SAFARI 2000 period and found very close agreement.

[4] The objective of this paper is to demonstrate the capability of MODIS to effectively observe and monitor different types of aerosols not only from a global perspective but also to meet specific regional objectives. Southern African regional aerosols are dominated by smoke, originating from biomass burning, which is a regular phenomenon in this region, especially during the August–September time frame. MODIS is the first operational satellite sensor with daily global coverage capable of measuring AOT at several wavelengths over land and ocean. Its unique ability to differentiate the contributions of coarse and fine mode aerosols to AOT, makes it ideal for sensing smoke aerosols, which belong to the fine mode. Section 2 presents an overview of the southern African regional characteristics and previous experiments. Section 3 describes briefly the MODIS aerosol retrieval process and data products, and section 4 discusses the data application in climate forcing calculations.

2. Background

[5] The southern African subcontinent has certain unique physical and meteorological characteristics, both of which influence the emission, transport, and climate forcing of aerosols. Most of southern Africa is dominated by the savanna type of ecosystem, changing to subtropical and tropical toward the north, and to semiarid and arid toward the southwest. As part of the agricultural practice in the region, the savanna vegetation is periodically subjected to extensive biomass burning. The intensity of this activity varies from season to season, and so does the corresponding emission of smoke aerosols and other particulates, ozone, and other trace gases [*Lindesay et al.*, 1996; *Swap et al.*, 1996]. Based on data acquired with the Total Ozone Monitoring Spectrometer (TOMS) and in situ measurements obtained during the Stratospheric Aerosol Gas Experiments (SAGE) between 1979 and 1989, *Fishman et al.* [1991] established that the southern African pollution maximum usually occurs during the austral spring (September to November). They further indicated that most of the pollution observed over southern Africa and the adjoining southern Atlantic regions originate from widespread biomass burning in the tropical and subtropical southern Africa. Indeed, during the austral spring, the dominant aerosol type over southern Africa and surrounding oceanic regions is smoke. During the rest of the year, when the biomass burning activity and the associated smoke emissions decrease, dust and industrial pollution become the dominating aerosol types, especially in summer and winter [*Piketh et al.*, 1999], although the overall aerosol concentration is considerably reduced. The seasonal variability of aerosol concentration over southern Africa is more strongly demonstrated by *Eck et al.* [2003] using AERONET measurements. Multiannual monthly averages of aerosol optical thickness at 550 nm wavelength measured over Mongu (Zambia) from 1995 to 2000 show September and April as the months with the highest and lowest aerosol loading, respectively.

[6] Southern Africa had been a focus of past intensive field campaigns. The Southern Tropical Atlantic Region Experiment (STARE), which took place in 1992, involved several ground-based and aircraft in situ measurement activities, and remote sensing, and hundreds of scientists from several countries participated [*Andreae et al.*, 1996]. STARE was composed of two complementary semi-independent campaigns; the Transport and Atmospheric Chemistry near the Equator-Atlantic (TRACE-A) and the Southern African Fire-Atmosphere Research Initiative (SAFARI). The objective of TRACE-A was "to investigate the emissions from the source regions in Brazil and the transport and photochemical processing of the emitted gases over the continent and the tropical South Atlantic" [*Andreae et al.*, 1996, p. 23,519], while that of SAFARI (hereafter referred to as SAFARI-92) was "to investigate the emissions from fires and soils in southern Africa, the meteorology over the subcontinent, and the ecological impact of fires in the African savannas" [*Andreae et al.*, 1996, p. 23,519]. Together, TRACE-A and SAFARI-92 covered the vast area extending across the southern Atlantic Ocean, from Brazil to southern Africa. The aim was "to characterize the emissions from biomass burning in the source regions on either side of the Atlantic, the transport of air masses from these source regions to the atmosphere over the Atlantic, and the chemical transformations occurring in the air masses" [*Lindesay et al.*, 1996, p. 23,522]. SAFARI-92 produced many interesting results from ground-based and airborne measurements in situ, as well as meteorological data, most of which were published in the STARE special issue of the Journal of Geophysical Research-Atmospheres (JGR, volume 101, number D19) on October 30, 1996. However, very limited results were derived from satellite sensors, because at that time, only TOMS and NOAA-AVHRR (Advanced Very High Resolution Radiometer) were operationally producing daily global coverage. The use of AVHRR data for active fire and burned area detection was described respectively by *Justice et al.* [1996] and *Scholes et al.* [1996], while the application of TOMS was typically focused on ozone monitoring [e.g., *Fishman et al.*, 1996; *Kim et al.*, 1996; *Thompson et al.*, 1996]. There was no satellite-based aerosol characterization specifically applied to SAFARI-92.

[7] The recent SAFARI 2000 field campaign, which took place in August and September 2000 constitutes a follow-up to the SAFARI-92 experiment. The introductory statement on the SAFARI 2000 web site describes the campaign as "an international regional science initiative being devel-

oped for southern Africa to explore, study and address linkages between land-atmosphere processes and the relationship of biogenic, pyrogenic or anthropogenic emissions and the consequences of their deposition to the functioning of the biogeophysical and biogeochemical systems of southern Africa'' http://safari.gecp.virginia.edu/index.asp). Great optimism was expressed on the potential role of the sensors aboard the EOS Terra satellite toward achieving the specific objectives of the experiment. Indeed, the availability of the Terra satellite and its five-sensor complement is one of the major advantages that SAFARI 2000 had over SAFARI-92. One of the core elements of the campaign, as outlined in the SAFARI 2000 science plan, was to characterize aerosol emissions, distribution, physical and chemical properties, as well as transport and deposition [*Swap et al.*, 2002]. Aerosol retrieval from space predate Terra. For instance, aerosol optical thickness is being retrieved and validated over ocean from AVHRR [e.g., *Husar et al.*, 1997; *Stowe et al.*, 1997; *Mishchenko et al.*, 1999; *Ignatov*, 2002; *Zhao et al.*, 2002], as well as over land and ocean from TOMS [e.g., *Torres et al.*, 2002], although both sensors have limited spectral capability and TOMS has a low spatial resolution. Aerosols are also retrieved from the Multiangle Imaging Spectro-Radiometer (MISR) onboard Terra, and specifically, results of MISR aerosol retrieval over southern Africa during SAFARI 2000 have been reported by *Diner et al.* [2001]. However, MISR's limited swath width prevents daily global coverage. MODIS, therefore, is unique among all existing satellite sensors in providing daily global characterization of aerosols over land and ocean, as well as retrieving AOT at both short and longer wavelengths (longer wavelengths only over ocean) and distinguishing between coarse and fine mode aerosols. In fact, many in situ ground-based or airborne aerosol measurements during SAFARI 2000 have been used to compare or validate MODIS aerosol retrievals, as reported in various papers published in this issue.

3. MODIS Aerosol Data

[8] This section summarizes the various aspects of the MODIS aerosol data generation, validation, and analysis. First, the underlying principles encoded in the retrieval algorithm are summarized. Then, the various structures of the different data sets are described. This is followed by a summary of the validation effort and the southern African results for the SAFARI 2000 period and beyond.

3.1. Basic Concepts of Aerosol Retrieval

[9] The principle of aerosol retrieval from MODIS hinges on the simple theory that, at the reflective wavelengths (443–2130 nm), the solar reflectance reaching the top of the atmosphere (TOA), which is what the satellite sensor measures, is approximately the sum of the reflectance from the surface and the atmosphere. This can be very simply expressed as follows:

$$\rho_\lambda^{toa} \sim \rho_\lambda^{surf} + \rho_\lambda^{atm}, \quad (1)$$

where, ρ_λ^{toa} is reflectance reaching the top of the atmosphere at wavelength λ, and ρ_λ^{surf} and ρ_λ^{atm} are, respectively, the surface and atmospheric components of the reflectance. Aerosol spectral reflectance can be used to derive information on aerosol type, which then can be used to derive the aerosol content. Therefore aerosol optical (and in some cases also size) parameters can be derived from ρ_λ^{atm} (also referred to as path radiance), based on the following simple relationship in the single scattering approximation:

$$\rho_\lambda^{atm} \sim \tau_{a\lambda} * \omega_{0\lambda} * P_\lambda(\theta), \quad (2)$$

where, $\tau_{a\lambda}$ is the aerosol optical thickness (AOT), $\omega_{0\lambda}$ is single scattering albedo (SSA), and $P_\lambda(\theta)$ is the phase function for scattering angle θ; all at wavelength λ. However, the satellite sensor measures only ρ_λ^{toa}, from which ρ_λ^{surf} needs to be subtracted to obtain the exact value of ρ_λ^{atm}. Since ρ_λ^{surf} is not known, it is estimated from other measurements or models. The degree of complexity and reliability of this estimation depends on whether the surface is ocean or land, and in the case of the latter, what the land-cover type is. This is why MODIS aerosol retrieval follows different procedures over ocean and over land. However, both procedures involve very intricate processes of data filtering, model fitting, error analysis, and pixel aggregation, which result in 10 × 10-km spatial resolution level 2 aerosol products. MODIS has a full complement of onboard calibrators and the ρ_λ^{toa} data used for aerosol retrieval are precalibrated. The MODIS calibration team assures the data quality, and thus far, the calibration results show that the signal-to-noise ratios (SNR) for the wavebands used for aerosol retrieval meet and exceed prelaunch estimates.

3.1.1. Principles of Retrieval Over Ocean

[10] Ocean surfaces are dark in the (550–2130 nm) wavelength range. Over ocean, the surface reflectance ρ_λ^{surf} surf can be expressed as:

$$\rho_\lambda^{surf} \sim \rho_\lambda^{we} + \rho_\lambda^{Fresnel} + \rho_\lambda^{foam}, \quad (3)$$

where, ρ_λ^{we} is water-leaving radiance, $\rho_\lambda^{Fresnel}$ is Fresnel reflection from sea-surface waves, and ρ_λ^{foam} is reflection by sea-surface foam. However, under normal conditions, ρ_λ^{surf} is small, and ρ_λ^{atm} is almost equal to the measured ρ_λ^{toa}. In the algorithm, aerosol optical thickness $\tau_{a\lambda}$ is not evaluated in real time from equation (2), as that would consume enormous amounts of computer time. Rather, prior to running the algorithm, lookup tables (LUT) are generated through radiative transfer calculations based on several aerosol models, for different values of essential parameters. Specifically, the parameters considered include: nine aerosol particle sizes (four in the small mode and five in the large mode), five $\tau_{a\lambda}$ values (0, 0.2, 0.5, 1.0, and 2.0) at 550 nm wavelength, 9 solar zenith angles, 16 satellite zenith angles, 16 relative Sun/satellite azimuth angles. Furthermore, ρ_λ^{we} = 0.005 is used at 550 nm while ρ_λ^{we} = 0 is assumed at other wavelengths. For calculating $\rho_\lambda^{Fresnel}$ and ρ_λ^{foam}, a constant average wind speed of 6.0 m/s is assumed. The use of this constant wind speed value does not affect the results significantly because, as *Gordon* [1997] pointed out, the residual effect of the wind speed is minimal outside of glint regions, which are currently not covered in the MODIS aerosol retrievals. Details of the theory and operational methodology of MODIS aerosol retrieval over ocean, including, cloud and glint screening, error analysis, and

quality assurance, are described by *Tanré et al.* [1997], while the characteristics of the updated version of the algorithm are described by *Levy et al.* [2003]. The aerosol parameters retrieved with the MODIS ocean algorithm include: AOT at 470, 550, 660, 870, 1200, 1600, and 2130 nm wavelengths; Ångstrom exponent (α); fraction (η) of $\tau_{a\lambda}$ contributed by small mode aerosol; and the effective radius of the dominant size mode r_{eff}. The prelaunch estimated accuracies were: $\Delta\tau_a = \pm 0.05 \pm 0.05\tau_a$ (at 550 nm), $\Delta\eta = \pm 0.25$, and $\Delta r_{eff} = 0.3 r_{eff}$ [*Tanré et al.*, 1997]. Subsequent field studies using airborne simulators [*Tanré et al.*, 1999] and the validation of actual MODIS aerosol retrieval over ocean [*Remer et al.*, 2002b] suggest even better accuracy for combustion-type aerosols. However, for dust aerosols, because of nonsphericity the accuracy is lower than prelaunch estimates [*Levy et al.*, 2003].

3.1.2. Principles of Retrieval Over Land

[11] Unlike ocean surfaces, land surfaces often have complex cover categories, with highly variable reflective properties, and it is difficult to make assumptions sufficiently comprehensive to compute ρ_λ^{surf} accurately. Therefore a different approach is employed in estimating ρ_λ^{atm} from the measured ρ_λ^{toa}. At 2130 nm wavelength, most aerosols are transparent, and ρ_{2130}^{atm} is assumed to be 0. Thus, from equation (1), $\rho_{2130}^{surf} \sim \rho_{2130}^{toa}$. Based on prior observational studies, *Kaufman et al.* [1997b] established that, for dark surfaces (dark dense vegetation or dark soils), reflectance at 2130 nm is twice that at 660 nm and four times that at 470 nm (i.e., $\rho_{2130}^{surf} = 2\rho_{660}^{surf}$ and $\rho_{2130}^{surf} = 4\rho_{470}^{surf}$). As such, ρ_λ^{surf} can be derived at 470 and 660 nm and used (together with the corresponding measured ρ_λ^{toa} at 470 and 660 nm) for the retrieval of $\tau_{a\lambda}$. The MODIS radiance (level 1B) data with spatial resolutions of 250 m (at 660 nm) and 500 m (at 470 and 2130 nm) are used for this purpose. In the MODIS aerosol land algorithm, dark pixels ($\rho_{2130} < 0.15$) are selected, and ρ_{660}^{surf} and ρ_{470}^{surf} are evaluated ($\rho_{660}^{surf} = {}^{\rho 2130toa}/_{2}$ and $\rho_{470}^{surf} = {}^{\rho 2130toa}/_{4}$). These are subtracted from ρ_λ^{toa} to derive ρ_λ^{atm} at 660 and 470 nm. Pixels representing water, shadows, clouds, snow, or ice are excluded, using appropriate masks.

[12] Once ρ_λ^{atm} is determined at 660 and 470 nm, the LUT approach is used for the rest of the retrieval, as in the ocean algorithm. However, as opposed to the ocean algorithm in which nine models are considered, the over-land aerosol algorithm uses only three models. Two of these are used for small mode aerosols (biomass burning smoke or urban/industrial pollution), while the third model represents dust, which belongs to the large mode. During the retrieval, first, the aerosol is identified as either "dust" or "nondust" based on the spectral dependence of ρ_λ^{atm} at 470 and 660 nm. If it is nondust, the algorithm identifies it as smoke or pollution based entirely on location and season. There is possibility of mixing coarse and fine mode aerosols, but not both smoke and pollution. The difference between the two fine modes is minimal at low AOT and slowly increases with AOT. Therefore, in the event of fine mode misidentification (i.e., if smoke is confused with pollution or vice versa), as long as the aerosol loading is low to moderate, the potential error incurred is within the expected uncertainty. Accurate small mode identification becomes more important at high aerosol loading. The algorithm matches ρ_λ^{atm} to values in the LUT for the appropriate aerosol models, and the corresponding aerosol parameters are retrieved. These parameters include AOT at 470, 550, and 660nm wavelength along with Ångstrom exponent. The complex process involved in the algorithm, including aerosol model selection and spatial and statistical pixel sampling, is properly detailed by *Kaufman et al.* [1997a]. The prelaunch accuracy estimates for MODIS aerosol retrieval over land was $\Delta\tau_{a\lambda} = \pm 0.05 \pm 0.20\tau_{a\lambda}$ [*Chu et al.*, 1998]. This accuracy has been confirmed post-launch with actual MODIS data [*Chu et al.*, 2002].

3.2. The MODIS Aerosol Products

[13] The primary MODIS aerosol products comprise the level 2 parameters retrieved at 10 × 10-km spatial resolution over land and ocean as described above. These are held in raster data files corresponding to the standard MODIS individual 5-min data segments covering areas of approximately 1354 km (across track) by 2030 km (along track). These level 2 products are operationally aggregated to generate global data products, referred to as level 3, at 1-degree spatial resolution, on a daily, 8-day (weekly), and monthly basis. These global products are very useful for spatially continuous visualization, evaluation, and modeling, either globally or regionally.

[14] Figure 1 shows: (a) MODIS true color composite image for 24 August 2000, generated from the radiance data (level 1B) at the visible wavelengths (RGB = 660, 550, and 470 nm), showing a greater part of southern Africa at 1-km spatial resolution; (b) corresponding retrieval of τ_{a550} at 10-km spatial resolution. The gap between two successive swaths can be seen traversing the center of the images. The gray areas in the τ_{a550} image (Figure 1b) do not have aerosol retrieval because of the adverse effects of excessive surface brightness or cloud cover.

[15] Figure 2 shows global monthly composites of τ_{a550} (level 3) for September 2000, and April and September 2001. The gray areas correspond to arid or ice/snow land-cover types, which have no aerosol retrieval because of surface properties outside the boundaries of the algorithm assumptions. September 2000 was the period of SAFARI 2000, and the significantly high concentration of aerosols over southern Africa relative to other parts of the world is very obvious. By contrast, the month of April 2001 shows practically no aerosol concentration (beyond background levels) over that region. By September 2001, the situation reverts back to high aerosol levels over southern Africa. This is supporting evidence that the peak of aerosol concentration over that region (and indeed over the entire southern hemisphere) occurs in the August-October (austral spring) time frame, as suggested in previous papers [*Fishman et al.*, 1991] and as demonstrated over Zambia with high quality AERONET data [*Eck et al.*, 2003]. Since that time of year also corresponds to the peak of biomass-burning activities in southern Africa, it implies that aerosols over that region originate mainly from fires.

3.3. Validation of MODIS Aerosol Products

[16] MODIS aerosol products have been subjected to continuous intensive and extensive validation since the first set of data were produced. The effort has been directed mainly at the 10-km resolution level-2 products, whose validation would imply that of the level 3 products as well,

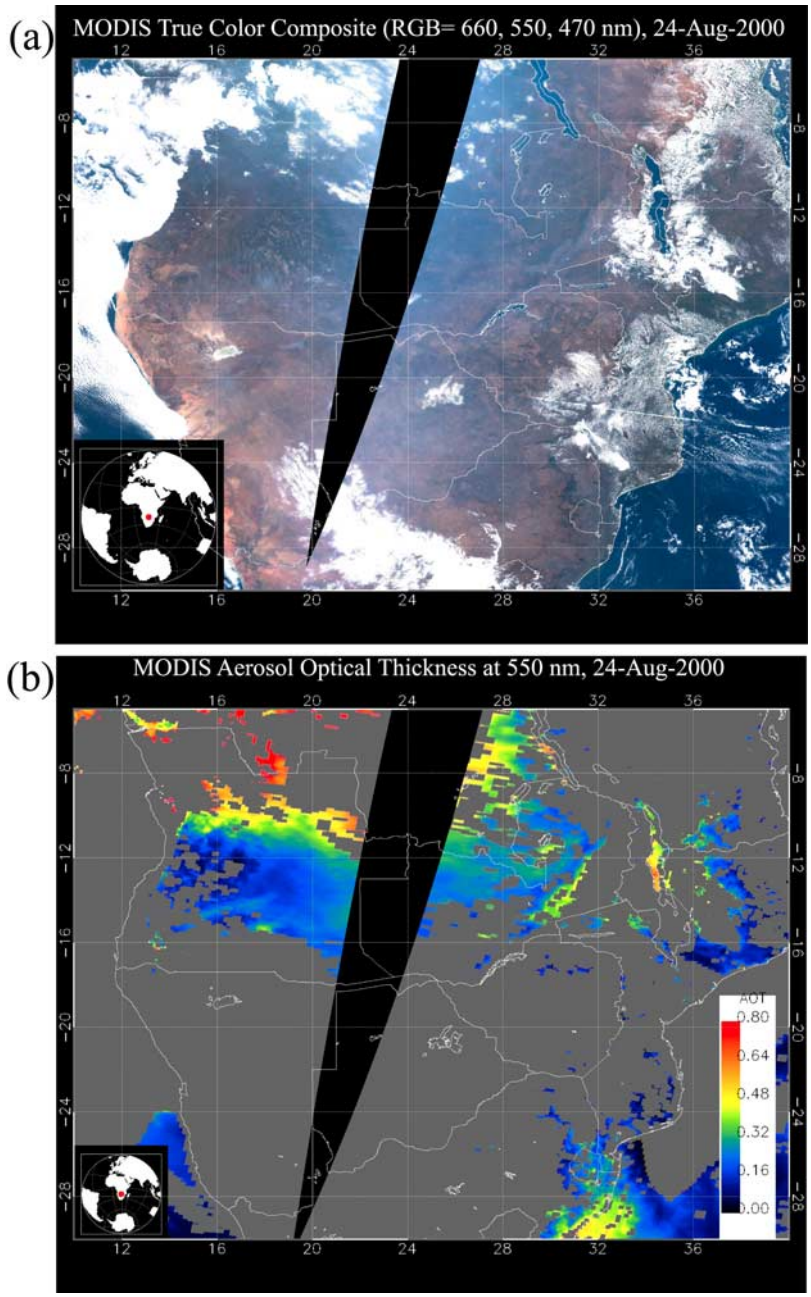

Figure 1. MODIS daily image products for 24 August 2000, covering the SAFARI- 2000 region: (a) True color composite (TCC) image generated from MODIS level 1B radiance data at 1-km spatial resolution with 660, 550, and 470 nm channels assigned to the red, green, and blue colors respectively; (b) Color-coded MODIS retrieved level 2 aerosol optical thickness (AOT) at 550 nm wavelength, with a spatial resolution of 10 km. The central near-vertical black gap on both images corresponds to the space between consecutive swaths. The remaining dark areas in the AOT image (Figure 1b) have no retrieval because of cloud cover or excessive surface brightness.

since the latter is simply an aggregation of the former. MODIS aerosol validation is accomplished mostly with measurements from ground-based AERONET (Aerosol Robotic Network) and other Sun photometers at individual point locations around the world. There are currently about two hundred validation sites in the MODIS aerosol validation database. It is obvious that MODIS aerosol data represent measurements of the parameter values over continuous areas once a day, while Sun photometers acquire measurements over point locations several times a day (approximately every 15 min for AERONET). To facilitate matching between the two data types for validation and other analytical purposes, a spatiotemporal technique was developed to generate statistics (spatial for MODIS and temporal from AERONET) of collocated points [*Ichoku et al.*, 2002]. For a given location, spatial statistics are computed from MODIS pixels within a 50 $\times$ 50-km box centered over the validation point, while temporal statistics

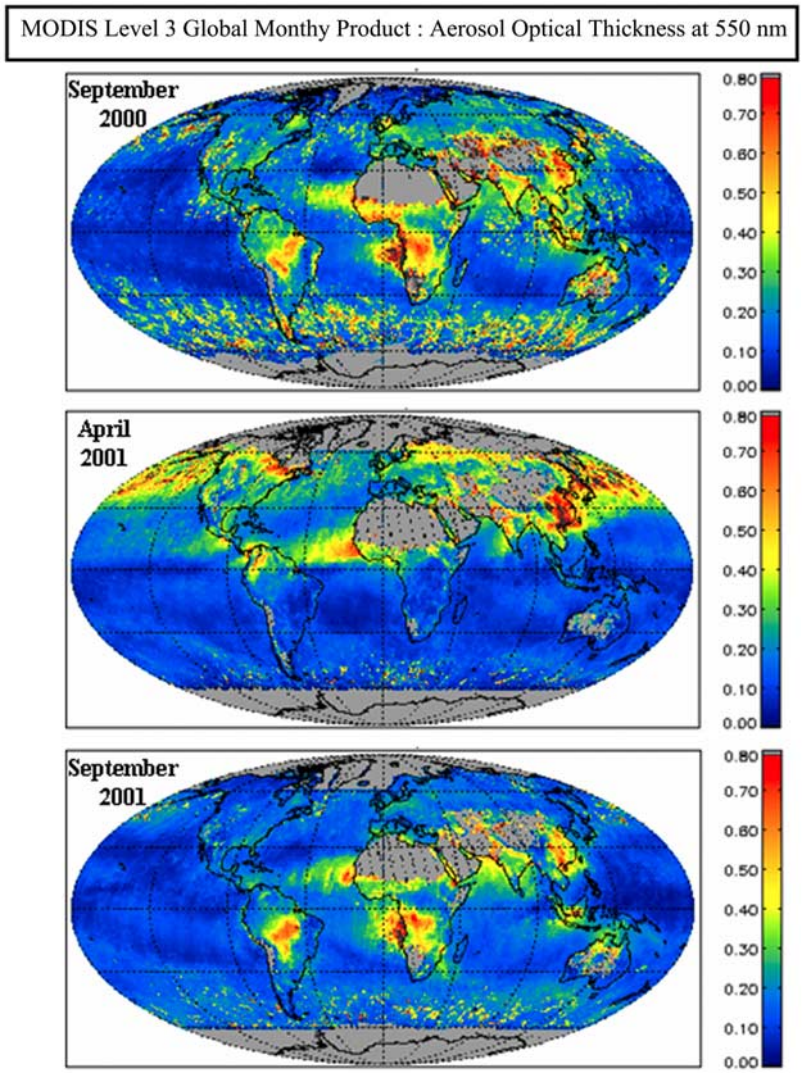

Figure 2. MODIS level 3 global monthly composites of aerosol optical thickness (AOT) at 550 nm showing heavy aerosol loading over southern Africa and the neighboring southern Atlantic Ocean during SAFARI 2000 in September 2000. Similar products for April and September 2001 are also shown for comparative purposes. The seasonality of the southern African aerosol loading due to biomass burning is clearly evident: high during September and very low around April. The SAFARI 2000 period also shows some aerosol overflow into West Africa.

are computed from AERONET data measured within ±30 min of the time of MODIS data acquisition. For the MODIS aerosol data (10 km spatial resolution), the 50 km box comprises 25 pixels, although because of clouds or other factors, not all pixels contain retrievals. Similarly, for AERONET, the one-hour interval would comprise 4 or 5 data points, though these could be fewer because of data gaps due to clouds or other factors. The computed MODIS spatial statistics are: mean, standard deviation, spatial slope, slope direction, and multiple correlation coefficient. The AERONET temporal statistics are: mean, standard deviation, temporal slope, and linear correlation coefficient.

[17] MODIS aerosol validation against AERONET involves the cross-correlation between corresponding statistical data sets. However, to ensure adequate data sampling, only statistical values computed from at least 20% or 2 valid values (whichever is larger) out of the total data sample are considered. This represents at least 5 (out of a maximum of 25) MODIS pixels and at least 2 (out of a maximum of 5) AERONET data points. Results of validation of MODIS aerosol products over land were presented by *Chu et al.* [2002], while *Remer et al.* [2002b] described validation over ocean. The AERONET data used in those validations were the level 1.5 cloud-screened data. Over land, scatterplots of $\tau_{a\lambda}$ between MODIS and AERONET based on data for July to September 2000 covering most validation points around the world, showed linear correlation coefficients of 0.91 and 0.85 at 470 nm and 660 nm wavelengths, respectively, with slopes equal to 0.86 and intercepts 0.02–0.06. Similar plots were generated for four different regions (Central USA, Europe, South America, and southern Africa) for the same time period, with results in the same range of values. Furthermore, in all cases, the MODIS aerosol retrievals over land were found to meet the expected

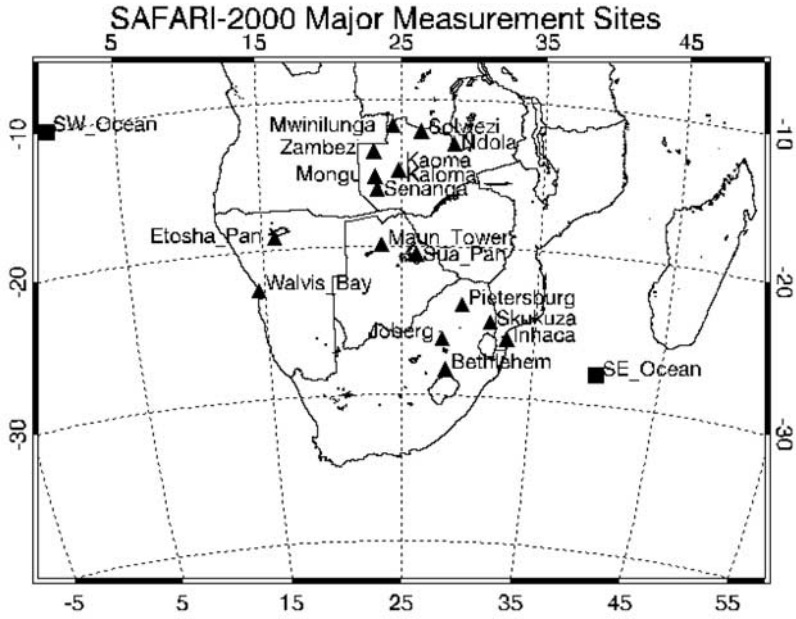

Figure 3. Location map showing major ground based measurement sites during SAFARI 2000. The sites on the subcontinent are indicated with solid triangles. Two additional sites, indicated with solid rectangles, are selected over the neighboring southern Atlantic and Indian oceans to study regional aerosol influences.

accuracy (errors within $\Delta\tau_{a\lambda} = \pm 0.05 \pm 0.20\tau_{a\lambda}$) [*Chu et al.*, 2002]. Similar linear fits performed with the over-ocean product produced a regression coefficient of $R = 0.94$ at 660 nm, with a slope of 1.01 and an intercept of 0.005. The data were well within the expected uncertainty ($\Delta\tau_{a\lambda} = \pm 0.03 \pm 0.05\tau_{a\lambda}$) [*Remer et al.*, 2002b]. Surface reflectance influences were demonstrated to be responsible for the slightly lower accuracy of the land retrievals (in contrast to ocean retrievals), especially at low $\tau_{a\lambda}$ values [*Ichoku et al.*, 2002].

3.4. MODIS Aerosol Products for Southern Africa

[18] Figure 3 shows a map of southern Africa, with the main land locations where ground measurements were conducted indicated with solid triangles. During SAFARI 2000, most of these continental sites were occupied by AERONET or other Sun photometers, as well as different kinds of other ground-based or airborne instrumentation, whose results are reported in other papers in this issue. Some of the locations, however, are long-term AERONET measurement sites. In addition, two locations (indicated with solid rectangles) have been selected on the neighboring oceans to the east and west of southern Africa for comparative studies, even though no ground-based or airborne measurements were conducted on them.

[19] Figure 4 shows scatterplots of $\tau_{a\lambda}$ for MODIS against AERONET at 470 and 660 nm wavelengths. They comprise all the available MODIS/AERONET collocated data, acquired during the months of August and September 2000, meeting the minimum sampling requirements of five MODIS pixels and two AERONET data points for the spatiotemporal statistics. It is pertinent to note that MODIS did not acquire data during the first half of August 2000 because of a technical problem. The data averages determine the point positions in the scatterplots, while the standard deviations are shown as error bars (note the difference in scale causing the error bars to appear longer at 660 nm). The diagonals represent the 1-to-1 lines. The data represent only four locations, which are distinguished with different markers. The two sites (Mongu and Zambezi) located in the north-central part of the region (within the country of Zambia) show larger aerosol concentrations, but incidentally, MODIS seems to underestimate $\tau_{a\lambda}$ with respect to AERONET over these sites, with the discrepancy increasing as AOT increases. Given that MODIS performs appreciably well at most other locations worldwide, this apparent underestimation over Zambia could be due to one or more of several reasons. However, when such inconsistency occurs, the two most obvious suspects are uncertainty in surface reflectance assumptions and aerosol model suitability for a given aerosol type over a given geographic location.

[20] As indicated by *Chu et al.* [2002] and demonstrated by *Ichoku et al.* [2002], from a global perspective, surface reflectance assumptions have a greater influence at low AOT values. On the other hand, *Chu et al.* [2002] reports that the uncertainty in aerosol model has a greater impact at high AOT values. Specifically, in MODIS smoke aerosol retrieval, the aerosol single-scattering albedo (ω_0) value of $\omega_0 = 0.90$ is assumed for locations and seasons where the aerosol is identified as biomass-burning smoke, such as southern Africa in August and September. *Chu et al.* [1998] investigated the use of different values of ω_0 for AOT retrieval, based on MODIS Airborne Simulator (MAS) data acquired over Brazil during the SCAR-B (Smoke, Carbon, Aerosol and Radiation-Brazil) campaign. They found that the effect of ω_0 is very significant at high aerosol loading (large values of AOT). Measurements conducted by *Reid et al.* [1998] in Brazil revealed substantial differences in ω_0

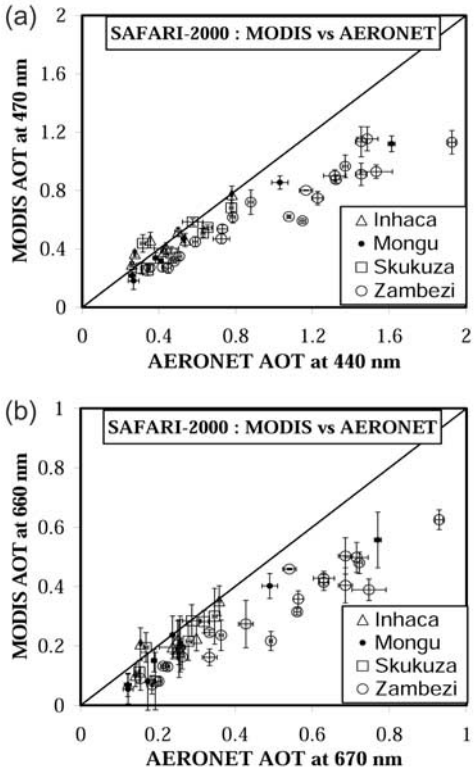

Figure 4. Scatterplots of SAFARI 2000 MODIS versus AERONET aerosol optical thickness (AOT) at: (a) 470 nm (MODIS) against 440 nm (AERONET) and (b) 660 nm (MODIS) against 670 nm (AERONET) wavelengths. They represent sites with sufficient data to meet the minimum spatiotemporal sampling requirements of the larger of 20% or 2 data points out of the total within the spatial (50 × 50 km) or temporal (1-hour) data window.

value between smoke aerosols generated from different ecosystems (cerrado and forest), as well as between young and aged smoke. In fact, based on in situ aircraft measurements over the cerrado (savanna-like) land-cover type, they found $\omega_0 = 0.79 \pm 0.04$ for local smoke and $\omega_0 = 0.85 \pm 0.02$ for aged smoke, both at 550 nm wavelength. *Eck et al.* [2001] compared ω_0 values derived from AERONET measurements for savanna biomass-burning smoke in southern Africa (Mongu, Zambia) and pasture/forest burning smoke in South America (Concepcion, Bolivia), and found a large difference between them. For τ_{a440} values ranging from 0.66 to 0.89, Mongu yielded ω_0 values of approximately 0.89, 0.83, and 0.80, while Concepcion gave 0.94, 0.92, and 0.91 at 440, 670, and 870 nm wavelengths respectively. In addition, using measurements acquired over a period of six years with AERONET Sun photometers at numerous locations around the world, *Dubovik et al.* [2002] derived the values of different aerosol optical properties, and classified them according to aerosol types and geographic regions. Their results show obvious differences in ω_0 between different regions even for the same aerosol type such as smoke. In particular, over the southern African savanna zone in Zambia, they found ω_0 to be 0.88, 0.84, 0.80, and 0.78 at 440, 670, 870, and 1020 nm wavelengths respectively, as contrasted with 0.91, 0.89, 0.87, and 0.85 over the Brazilian cerrado site.

[21] One important lesson learned here is that a single value of ω_0 is probably inadequate for global smoke aerosol retrieval. Even over southern Africa, the variability in ecosystems and types of biomass burned, and the variability in age of the smoke particles requires a variety of ω_0 for proper local aerosol retrievals. Areas such as Zambia appear to require smaller values of ω_0 than the $\omega_0 = 0.90$ used elsewhere. The MODIS aerosol products are a global product and cannot be fine-tuned for local conditions. Thus it becomes important to find a general value for ω_0 that can be applied reasonably well for the entire southern African subcontinent. From the values reported in the literature, as discussed above, and from a theoretical analysis, discussed below, it appears that a lower value than the current value of 0.90 will better represent ω_0 in the MODIS algorithm for southern Africa.

[22] The suitability of different values of ω_0 for MODIS smoke retrieval over southern Africa has been investigated through radiative transfer calculations, using relevant parameters corresponding to the SAFARI 2000 data plotted in Figure 4. For each of the two wavelengths (470 and 660 nm), different combinations of solar and sensor zenith angles, relative azimuth angle, and surface reflectance, were used to model the path radiance values (ρ_λ^{atm}) corresponding to the range of the retrieved aerosol optical thickness ($\tau_{a\lambda}$) for different single scattering albedos (ω_0). These calculations permitted a transformation of $\tau_{a\lambda}$ retrieved with $\omega_0 = 0.90$ to equivalent $\tau_{a\lambda}$ values, which MODIS would have retrieved if other ω_0 values were used instead. Figure 5 shows a reproduction of the MODIS versus AERONET τ_{a470} and τ_{a660} plots of Figure 4 (points represented with pluses, without trying to distinguish between locations). The solid curve corresponds to the value of $\omega_0 = 0.90$ used in the operational retrieval. For each wavelength, transformations of the points for the ω_0 value that brings them closer to the 1-to-1 line ($\omega_0 = 0.87$ at 470 nm and $\omega_0 = 0.85$ at 660 nm) are shown (black dots) together with theoretical curves for the same ω_0 values (dotted lines). In addition, the theoretical curves (broken lines) for the remaining two ω_0 values (in each case) are shown without their corresponding points, just for comparative purposes.

[23] Figure 5 shows the variability of ω_0 with increasing aerosol optical thickness. At 470 nm, when $\tau_{a470} \ll 1$, $\omega_0 = 0.90$ is suitable for maintaining close agreement between MODIS and AERONET. However, when $\tau_{a470} \sim 1$, $\omega_0 = 0.87$ to 0.88 is required to bring the points close to the 1-to-1 line, while for much larger values of τ_{a470}, slightly smaller ω_0 values (0.85–0.86) may be needed to bring the points up to the 1-to-1 line. At 660 nm, a single value of ω_0, ($\omega_0 = 0.85$) appears to be suitable to bring MODIS retrievals into close agreement with those of AERONET, at least for $\tau_{a660} \leq 1$. The slight curvature of the best fitting curves at 470 nm and the absence of curvature at 660 nm could be because of one or more of the following reasons: higher range of AOT values at 470 nm, difference in the variation of ω_0 with $\tau_{a\lambda}$, or multiple scattering effects. The MODIS Aerosol Science Team is currently studying these new results very closely, and plans to extend the investigation to other biomass-burning aerosol regions. This will enable

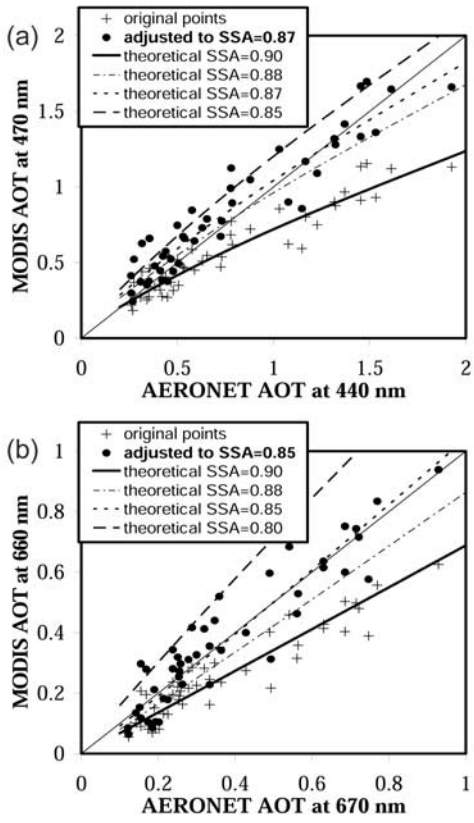

Figure 5. Scatterplots of SAFARI 2000 MODIS versus AERONET aerosol optical thickness (AOT) at the blue (440, 470 nm) and red (670, 660 nm) wavelengths. The pluses represent the AOT retrieved by MODIS using the single scattering albedo (SSA) value of $\omega_0 = 0.90$ (as shown in Figure 4, but without distinguishing between locations). At each wavelength, the four curves are theoretical calculations of MODIS retrievals using various ω_0 values. The solid curve corresponds to the value of $\omega_0 = 0.90$ used in the operational retrieval. The black dots represent the MODIS AOT retrievals adjusted to $\omega_0 = 0.87$ and 0.85 for the blue and red wavelengths, respectively. The diagonal is the 1:1 line.

the determination of suitable ω_0 values for implementation in future algorithm updates, in order to improve the accuracy of MODIS smoke aerosol retrieval in southern Africa and other affected areas.

[24] The long-term variation of aerosol concentration over southern Africa can be visualized using time series of MODIS spatial statistics (Figure 6) over four (Maun_Tower, Mongu, Ndola, Skukuza) well-distributed locations (refer to Figure 3). Plots representing two ocean locations (SW_Ocean and SE_Ocean) on either side of the subcontinent are also shown for comparative purposes and to assess the influence of the southern African biomass burning activities over the neighboring oceans. The plots show the means of the MODIS 50 × 50-km spatial subsets, with the corresponding standard deviations plotted as error bars. A five-point running average trend line is shown for each plot. It is pertinent to mention that part of the data acquired prior to August 2000 have not been well calibrated and should be interpreted with care. One common feature of all the plots in Figure 6 is that, as mentioned previously, major peaks of aerosol concentration occur mainly during the August–October time period each year (in this case, both in 2000 and 2001). It is interesting that the ocean sites showed no deficiency in aerosol loading, even though they are completely remote from all the possible smoke aerosol sources. This is indicative of the large scope of air circulation in the region. *Garstang et al.* [1996] presented a detailed study of the horizontal and vertical air transport

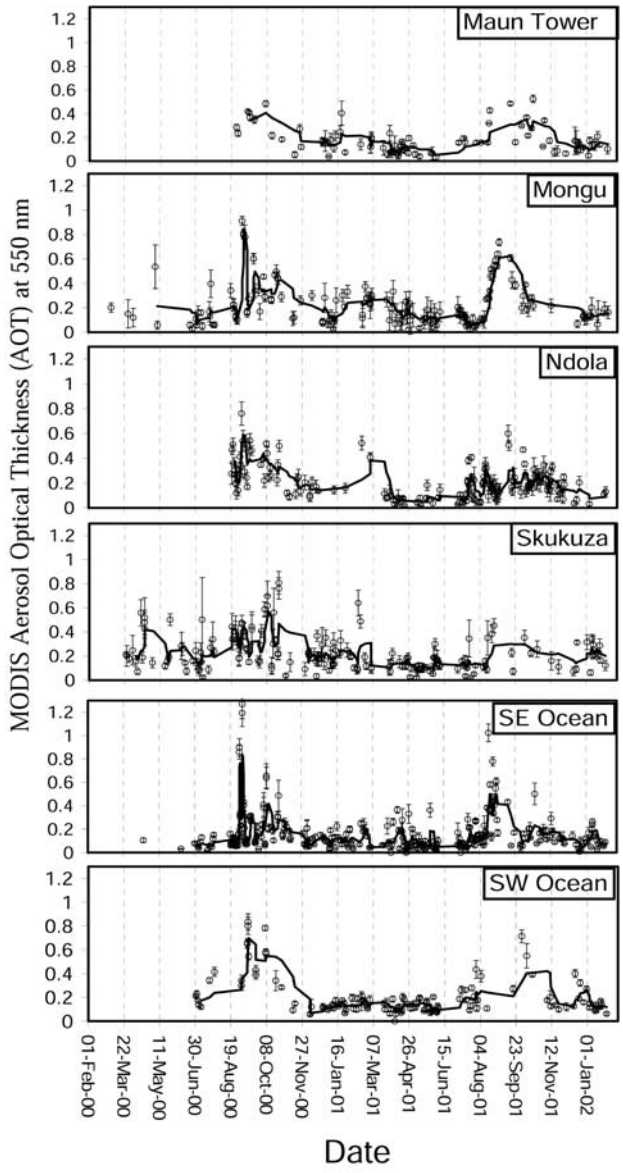

Figure 6. Long-term time series of the 50 × 50 km spatial averages of MODIS AOT at 550 nm wavelength over four continental sites (Maun_Tower, Mongu, Ndola, and Skukuza) and two oceanic sites (arbitrarily designated as SW_Ocean and SE_Ocean) shown on Figure 3. The means determine the positions of the points along the *y* axis, while the standard deviations are plotted as error bars. Five-point moving average trend lines are superimposed. Note that part of the data acquired prior to August 2000 have not been well calibrated and should be interpreted with care.

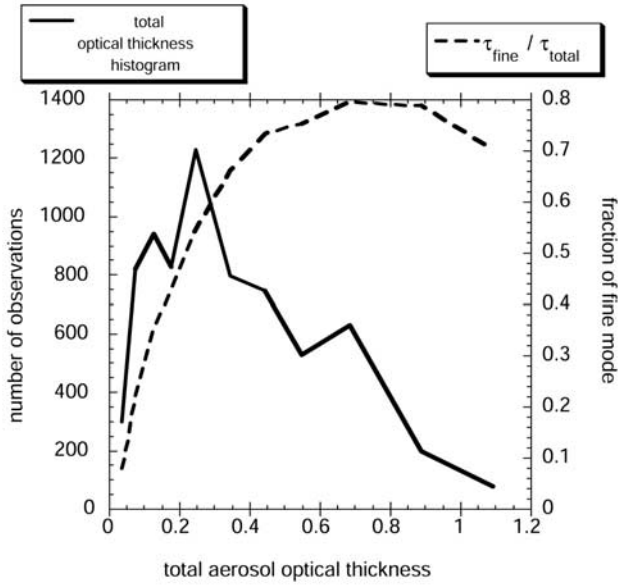

Figure 7. Total aerosol optical thickness histogram (solid line and left axis) and fraction of fine mode contribution to total aerosol optical thickness (dashed line and right axis) as functions of total aerosol optical thickness. These statistics derived from 7106 total observations of MODIS level 3 1° data located over the ocean regions in an area defined between 15°W and 30°E, from the equator to 20°S during the month of September 2000.

over southern Africa during the SAFARI-92 campaign. They noted that the high concentrations of aerosols over the subcontinent as well as over the tropical South Atlantic and southwestern Indian Oceans in winter and spring are caused by a distinctive suite of transport patterns resulting from the integrated effects of controls exerted by atmospheric stability on vertical mixing and the nature of the horizontal circulation fields. In Figure 6, it is also important to highlight the secondary peaks noticable for Ndola (and slightly also for Mongu and Skukuza) occurring around March and April, which are likely due to "crustally derived aeolian dust and industrially produced sulphur aerosols" demonstrated as being the major summer and winter constituents of the haze layer over southern Africa [*Piketh et al.*, 1999].

4. Southern African Regional Aerosol Impact Assessment From MODIS

[25] The high levels of aerosol optical thickness $\tau_{a\lambda}$ observed over southern Africa during SAFARI 2000, and at other times, create a strong surface and top of the atmosphere (TOA) aerosol forcing. The MODIS ability to separate fine and coarse mode aerosol optical thickness allows us to calculate this forcing using, for instance, the monthly data for September 2000 (Figure 2). Focusing on the ocean part of the region within the boundaries from 15°W to 30°E and from the equator down to 20°S, we construct a histogram of $\tau_{a\lambda}$ values for the entire ocean region from the 1° resolution level 3 AOT data at 550 nm wavelength. Note that we rely on the general results of *Remer et al.* [2002b] for validation of the ocean $\tau_{a\lambda}$ retrievals and subsequent histogram, because the specific validation shown in Figure 4 was done exclusively with MODIS retrievals over land (not ocean). For each bin of this histogram we calculate the mean contribution from the fine and coarse modes. The histogram and the fine mode fraction of the total aerosol optical thickness are shown in Figure 7. The aerosol at low optical thickness consists mainly of a coarse mode, but shifts to 70–80% fine mode at higher optical thickness. This corresponds to a sea salt dominated regime that becomes overwhelmed by intrusions of heavy smoke aerosol. A total of 7106 observations were collected

Table 1. Input Parameters and Results of Flux Calculations Using the CLIRAD-SW Model for Standard SAFARI Parameters and Nine Other Perturbations to These Parameters[a]

Run	1	2	3	4	5	6	7	8	9	10 Best
					Input Parameters[b]					
Surface albedo	0.06	0.06	0.06	0.06	[0.05]	[0]	[0.3]	0.06	0.06	0.06
Profiles	mls	mls	mls	[Cui]	mls	mls	mls	mls	mls	mls
r_eff, μm, fine	0.20	0.20	0.20	0.20	0.20	0.20	0.20	[0.15]	0.20	0.20
r_eff, μm, coarse	1.0	1.0	1.0	1.0	1.0	1.0	1.0	1.0	[1.5]	1.0
ω_o, uv	0.9	[0.95]	[0.88]	0.9	0.9	0.9	0.9	0.9	0.9	[0.90/0.98]
ω_o, vis	0.865	[0.93]	0.865	0.865	0.865	0.865	0.865	0.865	0.865	[0.865/0.98]
ω_o, nir	0.82	[0.91]	0.82	0.82	0.82	0.82	0.82	0.82	0.82	[0.82/0.97]
ω_o, mir	0.705	[0.85]	[0.8]	0.705	0.705	0.705	0.705	0.705	0.705	[0.705/0.96]
					Results,[c] Wm^{-2}					
dF/dτ up TOA	33	43	34	33	35	42	−4	38	33	34
dF/dτ down surface	−103	−81	−103	−104	−103	−103	−75	−104	−103	−101
Difference up TOA	9	12	9	9	10	12	−1	10	9	10
Difference down surface	−27	−21	−27	−27	−27	−27	−25	−27	−27	−26

[a]Perturbations are enclosed in brackets.

[b]Input parameters: Profiles are taken either from a midlatitude summer (mls) atmosphere or measured profiles from Cuiaba, Brazil in 1995 (Cui). r_eff fine and r_eff coarse are the effective radii for the fine and coarse modes, respectively. ω_o is the single scattering albedo for the ultraviolet (uv), visible (vis), near infrared (nir) and mid infrared (mir) ranges of the solar spectrum.

[c]Results: All fluxes in Wm^{-2}. Net TOA and net surface are the net fluxes at the top and bottom of the atmosphere, respectively. Positive upward. Up TOA is the upwelling flux at top of atmosphere. Down surface is the downwelling flux at the surface. dF/dτ is the aerosol forcing per unit optical thickness. Difference is the total aerosol forcing for the region assuming MODIS-viewed aerosol optical thickness in the 0–0.10 range represents background conditions.

for the period, and the monthly mean AOT value for this region was 0.31 at 550 nm.

[26] We use the CLIRAD-SW (Climate Radiation-Shortwave) solar radiative transfer model [*Chou and Suarez*, 1999] to perform the flux calculations. The model includes water vapor, O_3, O_2, CO_2, clouds and aerosols, although we run it only for noncloudy conditions. Reflection and transmission are computed using the δ-Eddington approximation, and the fluxes are then computed using the two-stream adding approximation. The fluxes are integrated for the entire particle-size spectrum from 0.175 μm to 10 μm. The aerosol optical properties of single scattering albedo ω_0, asymmetry parameter g, and optical thickness $\tau_{a\lambda}$ are the inputs to the model. Because we have separate optical thickness values for fine and coarse mode, we can run the code multiple times, one set with optical properties applicable to the fine mode and another set with optical properties applicable to the coarse mode. The results are combined using the ratio of fine to total optical thickness as a weighting factor.

[27] Table 1 gives the input parameters used in the flux calculations. Single scattering albedo (ω_0) values in the visible and near infrared bands are estimated from *Dubovik et al.* [2002]. The single scattering albedo ω_0 is linearly extrapolated to the ultra violet and mid infrared parts of the spectrum. For most of the model runs we use the same set of ω_0 for both the fine and coarse mode. However, in our last model run, which we designate as our best estimate, we allow the two modes to have different ω_0 properties. Asymmetry parameter g is calculated from the MODIS aerosol models used in the over-ocean algorithm. The retrievals suggest a fine mode model with effective radius of 0.20 μm and a coarse mode model representing sea salt with effective radius of 1.0 μm. We use a surface albedo of 0.06, corresponding to ocean surface albedo, a midlatitude summer atmosphere and a solar zenith angle of 60°.

[28] The resulting flux calculations for our "best" estimate for each histogram bin are shown in Figure 8, plotted as a function of total aerosol optical thickness. As optical thickness increases, the upwelling flux at the top of atmosphere (solid line) increases, and more sunlight is scattered back to space. However, the downwelling flux at the surface (dashed line) decreases due to absorption by the aerosols. The slopes of the lines give the forcing per unit optical thickness. The surface response is roughly three times stronger than that at the top of the atmosphere.

[29] Another way to calculate the aerosol forcing is to take the fluxes in all histogram bins and sum them, after weighting the value in each bin by its frequency of occurrence of MODIS observations. This produces the total monthly fluxes for the region. The aerosol forcing portion of these fluxes is found by subtracting out the fluxes due to background conditions. Estimating background aerosol can be a large source of error when deriving anthropogenic forcing from satellite measurements [*Remer et al.*, 2002a]. *Kaufman et al.* [2001] determined the background aerosol optical thickness over the world's oceans to be 0.05–0.07. These values fall within the first two bins of the optical thickness histogram of Figure 7. Therefore we assume that background conditions are represented by an average of the two bins with the smallest optical thickness. These results show that our best estimate

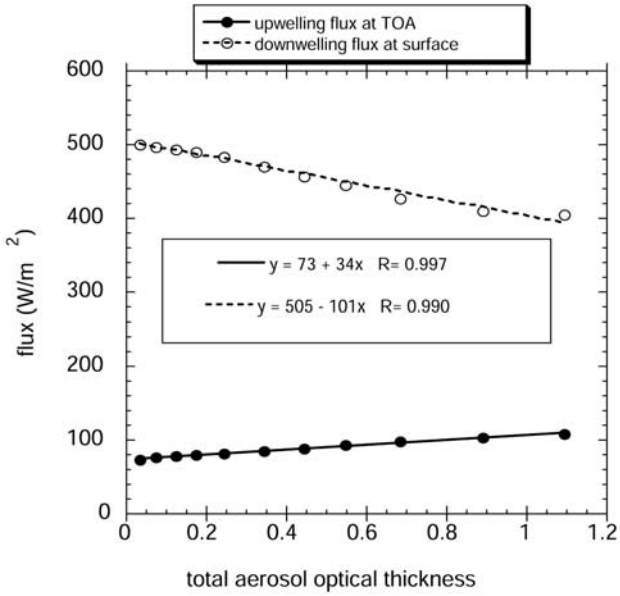

Figure 8. Calculations of upwelling flux at the top of the atmosphere (solid points and line) and downwelling flux at the surface (open points and dashed line) as functions of total aerosol optical thickness. Calculations were performed using MODIS-derived fine and coarse mode components of the total aerosol optical thickness. Input parameters are given in Table 1 for run 10, labeled "best."

of the forcing at the top of atmosphere is -10 Wm^{-2}, while the forcing at the surface is -26 Wm^{-2}. Assuming, instead, that background conditions are represented by the first histogram bin alone, these estimates of aerosol radiative forcing increase to -11 Wm^{-2} and -28 Wm^{-2}, respectively. The surface forcing is roughly 2.5 times stronger than that at the top of the atmosphere. These results are similar to the INDOEX results [*Satheesh and Ramanathan*, 2000; *Rajeev and Ramanathan*, 2001]. Also, *Christopher and Zhang* [2002] obtained good correlation between the MODIS-retrieved AOT and the shortwave aerosol radiative forcing derived from the CERES (Cloud and Earth's Radiant Energy System) sensor onboard the same Terra platform as MODIS. However, the coarse spatial resolution of CERES (30 km at nadir) and the associated cloud screening procedure prevented it from observing the large smoke plumes off the southern African Atlantic coast during the SAFARI 2000 period [*Christopher and Zhang*, 2002], resulting in some disagreement in the radiative forcing results between CERES and MODIS.

[30] The sensitivity of the MODIS results to our initial assumptions were tested by changing the values of certain input parameters during different runs of the radiative transfer code. The results of our sensitivity tests are provided in Table 1. The forcing at the top of the atmosphere is most sensitive to drastic changes in surface albedo, representing a calculation over a bright land surface (run 7). In terms of reasonable perturbations for ocean conditions, the forcing is mostly sensitive to the choice of the single scattering albedo in the visible and near infrared ranges of the spectrum (run 2), but less so to changes in the ultra

violet and mid infrared ranges (run 3). The sensitivity to single scattering albedo is strongest for the flux at the surface. Run 2 uses single scattering albedos derived for the deforestation regions of Brazil [*Dubovik et al.*, 2002]. Run 10, our best estimate, is the only run in which we designate different single scattering albedos for fine and coarse modes. The fine mode set is the same as run 1, representing values for southern African biomass burning, while the coarse mode set represents values for maritime aerosol [*Dubovik et al.*, 2002]. The sensitivity to the fine and coarse mode effective radii (r_eff), which also implies sensitivity to phase function and asymmetry parameter, is limited, as shown under runs 8 and 9 respectively.

[31] This study in calculating the aerosol direct forcing over the adjoining oceans of the SAFARI 2000 region demonstrates the power of the new MODIS products in determining important parameters that affect climate. The combination of MODIS accuracy, coverage and the ability to separate fine and coarse modes make this calculation substantially advanced over previous attempts with other satellites. Even so, these results should be viewed as a rough first approximation. In the future, forcing calculations can be computed directly from the MODIS-derived spectral fluxes, which are expected to be more accurate than the derivations of optical thickness. Furthermore, with the help of models, even greater accuracy and understanding of the processes can be achieved.

5. Conclusions

[32] Aerosol properties, including optical thickness and size parameters, are retrieved operationally from the MODIS sensor onboard the Terra satellite launched on 18 December 1999. Southern Africa experiences dust, smoke, and pollution aerosols in different proportions depending on season. During the southern hemisphere spring, the predominant aerosol type over the region is smoke, which is generated from biomass burning on land and transported over the southern Atlantic and Indian Oceans. The SAFARI 2000 period experienced substantial smoke aerosol emissions because it corresponded with the peak season for biomass burning activities in southern Africa.

[33] The MODIS Aerosol Science Team formulates and implements strategies for the retrieval and validation of aerosol products from MODIS. The aerosol products are further used to estimate aerosol effects in the radiative forcing of climate as accurately as possible. These activities are carried out not only from a global perspective, but also with a focus on specific regions identified as having interesting characteristics, such as the biomass burning phenomenon in southern Africa and the associated smoke aerosol, particulate, and trace gas emissions. Indeed, the SAFARI 2000 aerosol measurements from the ground and from aircraft, along with MODIS, provide excellent data sources for a more intensive and closer study of the aerosol characteristics over southern Africa.

[34] The SAFARI 2000 ground-based measurements of aerosol optical thickness (AOT) from the automatic Aerosol Robotic Network (AERONET) Sun photometers have been used to validate MODIS retrievals, based on a sophisticated spatiotemporal technique. Through this process it has been discovered that, during the biomass burning season, MODIS underestimates AOT with respect to AERONET over southern Africa. This phenomenon was observed particularly over Zambian locations. The discrepancy is attributed to the use of a constant value of $\omega_0 = 0.90$, derived over Brazil during SCAR-B in August–September 1995, for smoke aerosol retrieval globally. It has been estimated from other measurements that, at the visible wavelengths, a lower value of about $\omega_0 = 0.86$ would be more applicable to southern African smoke, and even at that, still lower values apply to fresh smoke with respect to aged smoke. Further studies are currently being conducted with a view to determining and applying more suitable values of ω_0 for aerosol retrieval over different regions of the globe, including southern Africa.

[35] The average global monthly distribution of aerosol from MODIS has been applied as input in a climate model to calculate the aerosol daily averaged (24 hr) radiative forcing for September 2000 over the ocean adjacent to southern Africa. It is estimated that, on the average, for cloud free conditions over an area of 9 million square km, this predominantly smoke aerosol exerts a forcing of approximately -26 W/m^2 close to the terrestrial surface and -10 W/m^2 at the top of the atmosphere (TOA). While cooling the surface and Earth system, the difference of 16 W/m^2 is energy that heats the atmosphere.

[36] From the foregoing analysis, it is obvious that MODIS has been, not only capable to provide data support to SAFARI 2000 and similar campaigns, but also accomplishes daily aerosol monitoring over southern Africa and the entire world. The capabilities continue to be investigated and expanded.

[37] **Acknowledgments.** We would like to thank the various MODIS software development and support teams for the production and distribution of the MODIS data. We specifically would like to express our sincere appreciation to Bill Ridgway and Rich Hucek for leading and coordinating the MODIS atmospheres production and distribution operations; Shana Mattoo for implementing the MODIS over-ocean aerosol algorithm and for valuable assistance in the radiative transfer calculations; Paul Hubanks for developing the MODIS level 3 atmosphere products and for maintaining the Web site; and Eric Moody and Mark Gray for developing relevant MODIS data subsetting and visualization tools, some of which were very useful for the data analysis. We also thank the AERONET team members, especially Ilya Slutsker, for collecting, processing, and making available ground-based aerosol observations around the world, and Tom Eck for very valuable comments on the initial version of this paper. Finally, we would like to acknowledge Ming-dah Chou and Max Suarez for their efforts in developing the CLIRAD model and encouraging its distribution.

References

Andreae, M. O., J. Fishman, and J. Lindesay, The Southern Atlantic Region Experiment (STARE): Transport and Atmospheric Chemistry Near the Equator-Atlantic (TRACE A) and Southern African Fire-Atmosphere Research Initiative (SAFARI): An introduction, *J. Geophys. Res.*, *101*, 23,519–23,520, 1996.

Chou, M.-D., and M. J. Suarez, A solar radiation parameterization (CLIRAD-SW) for atmospheric studies. *NASA/TM-1999-104606*, *15*, 48 pp., NASA, Greenbelt, Md., 1999.

Christopher, S. A., and J. Zhang, Shortwave aerosol radiative forcing from MODIS and CERES observations over the oceans, *Geophys. Res. Lett.*, *29*(18), 1859, doi:10.1029/2002GL014803, 2002.

Chu, D. A., Y. J. Kaufman, L. A. Remer, and B. N. Holben, Remote sensing of smoke from MODIS airborne simulator during the SCAR-B experiment, *J. Geophys. Res.*, *103*, 31,979–31,987, 1998.

Chu, D. A., Y. J. Kaufman, C. Ichoku, L. A. Remer, D. Tanré, and B. N. Holben, Validation of MODIS aerosol optical depth retrieval over land, *Geophys. Res. Lett.*, *29*(12), 8007, doi:10.1029/2001GL013205, 2002.

Diner, D. J., et al., MISR aerosol optical depth retrievals over southern Africa during the SAFARI 2000 dry season campaign, *Geophys. Res. Lett.*, *28*, 3127–3130, 2001.

Dubovik, O., B. N. Holben, T. F. Eck, A. Smirnov, Y. J. Kaufman, M. D. King, D. Tanré, and I. Slutsker, Variability of absorption and optical properties of key aerosol types observed in worldwide locations, *J. Atmos. Sci.*, *59*, 590–608, 2002.

Eck, T. F., B. N. Holben, D. E. Ward, O. Dubovik, J. S. Reid, A. Smirnov, M. M. Mukelabai, N. C. Hsu, N. T. O'Neill, and I. Slutsker, Characterization of the optical properties of biomass burning aerosols in Zambia during the 1997 ZIBBEE field campaign, *Geophys. Res.*, *106*, 3425–3448, 2001.

Eck, T., et al., Variability of biomass burning aerosol optical characteristics in southern Africa during the SAFARI 2000 dry season campaign and a comparison of single scattering albedo estimates from radiometric measurements, *J. Geophys. Res.*, *108*(D13), 8477, doi:10.1029/2002JD002321, 2003.

Fishman, J., K. Fakhruzzaman, B. Cros, and D. Nganga, Identification of widespread pollution in the Southern Hemisphere deduced from satellite analyses, *Science*, *252*, 1693–1696, 1991.

Fishman, J., V. G. Brackett, E. V. Browell, and W. B. Grant, Tropospheric ozone derived from TOMS/SBUV measurements during TRACE A, *J. Geophys. Res.*, *101*, 24,069–24,082, 1996.

Garstang, M., P. D. Tyson, R. Swap, M. Edwards, P. Kållberg, and J. A. Lindesay, Horizontal and vertical transport of air over southern Africa, *J. Geophys. Res.*, *101*, 23,721–23,736, 1996.

Gordon, H. R., Atmospheric correction of ocean color imagery in the Earth Observing System era, *J. Geophys. Res.*, *102*, 17,081–17,106, 1997.

Holben, B. N., et al., AERONET—A federated instrument network and data archive for aerosol characterization, *Rem. Sens. Environ.*, *66*, 1–16, 1998.

Holben, B. N., et al., An emerging ground-based aerosol climatology: aerosol optical depth from AERONET, *J. Geophys. Res.*, *106*, 12,067–12,097, 2001.

Husar, R. B., J. M. Prospero, and L. L. Stowe, Characterization of tropospheric aerosols over the oceans with the NOAA advanced very high resolution radiometer optical thickness operational product, *J. Geophys. Res.*, *102*, 16,889–16,909, 1997.

Ichoku, C., D. A. Chu, S. Chu, Y. J. Kaufman, L. A. Remer, D. Tanré, I. Slutsker, and B. N. Holben, A spatio-temporal approach for global validation and analysis of MODIS aerosol products, *Geophys. Res. Lett.*, *29*(12), 8006, doi:10.1029/2001GL013206, 2002.

Ignatov, A., Sensitivity and information content of aerosol retrievals from the advanced very high resolution radiometer: radiometric factors, *Appl. Opt.*, *4*, 991–1011, 2002.

Justice, C. O., J. D. Kendall, P. R. Dowty, and R. J. Scholes, Satellite remote sensing of fires during the SAFARI campaign using NOAA advanced very high resolution radiometer data, *J. Geophys. Res.*, *101*, 23,851–23,863, 1996.

Kaufman, Y. J., D. Tanré, L. A. Remer, E. F. Vermote, A. Chu, and B. N. Holben, Operational remote sensing of tropospheric aerosol over land from EOS moderate resolution imaging spectroradiometer, *J. Geophys. Res.*, *102*, 17,051–17,067, 1997a.

Kaufman, Y. J., A. Wald, L. A. Remer, B.-C. Gao, R. R. Li, and L. Flynn, The MODIS 2.1 μm channel—Correlation with visible reflectance for use in remote sensing of aerosol, *IEEE Trans. Geosci. Remote Sens.*, *35*, 1286–1298, 1997b.

Kaufman, Y. J., A. Smirnov, B. N. Holben, and O. Dubovik, Baseline maritime aerosol: Methodology to derive the optical thickness and scattering properties, *Geophys. Res. Lett.*, *28*, 3251–3254, 2001.

Kim, J. H., R. D. Hudson, and A. M. Thompson, A new method of deriving time-averaged tropospheric column ozone over the tropics using total ozone mapping spectrometer (TOMS) radiances: Intercomparison and analysis using TRACE A data, *J. Geophys. Res.*, *101*, 24,317–24,330, 1996.

Levy, R. C., L. A. Remer, D. Tanre, Y. J. Kaufman, C. Ichoku, B. N. Holben, J. Livingston, P. Russell, and H. Maring, Evaluation of the MODIS retrievals of dust aerosol over the ocean during PRIDE, *J. Geophys. Res.*, *108*, doi:10.1029/2002JD002460, in press, 2003.

Lindesay, J., M. O. Andreae, J. G. Goldammer, G. Harris, H. J. Annegarn, M. Garstang, R. J. Scholes, and B. W. van Wilgen, International Geosphere-Biosphere Programme/International Global Atmospheric Chemistry SAFARI-92 field experiment: Background and overview, *J. Geophys. Res.*, *101*, 23,521–23,530, 1996.

Mishchenko, M. I., I. V. Geogdzhayev, B. Cairns, W. B. Rossow, and A. A. Lacis, Aerosol retrievals over the ocean by use of channels 1 and 2 AVHRR data: Sensitivity analysis and preliminary results, *Appl. Opt.*, *38*, 7325–7341, 1999.

Piketh, S. J., H. J. Annegarn, and P. D. Tyson, Lower tropospheric aerosol loadings over South Africa: The relative contribution of aeolian dust, industrial emissions, and biomass burning, *J. Geophys. Res.*, *104*, 1597–1607, 1999.

Rajeev, K., and V. Ramanathan, Direct observations of clear-sky aerosol radiative forcing from space during the Indian Ocean Experiment, *J. Geophys. Res.*, *106*, 17,221–17,236, 2001.

Reid, J. S., P. V. Hobbs, R. J. Ferek, D. R. Blake, J. V. Martins, M. R. Dunlap, and C. Liousse, Physical, chemical, and optical properties of regional hazes dominated by smoke in Brazil, *J. Geophys. Res.*, *103*, 32,059–32,080, 1998.

Remer, L. A., Y. J. Kaufman, Z. Levin, and S. Ghan, Model assessment of the ability of MODIS to measure top-of-atmosphere direct radiative forcing from smoke aerosols, *J. Atmos. Sci.*, *59*, 657–667, 2002a.

Remer, L. A., et al., Validation of MODIS aerosol retrieval over ocean, *Geophys. Res. Lett.*, *29*(12), 8008, doi:10.1029/2001GL013204, 2002.

Satheesh, S. K., and V. Ramanathan, Large differences in tropical aerosol forcing at the top of the atmosphere and Earth's surface, *Nature*, *405*, 60–63, 2000.

Scholes, R. J., J. D. Kendall, and C. O. Justice, The quantity of biomass burned in southern Africa, *J. Geophys. Res.*, *101*, 23,667–23,676, 1996.

Stowe, L. L., A. M. Ignatov, and R. R. Singh, Development, validation, and potential enhancements to the second-generation operational aerosol product at the National Environmental Satellite, Data, and Information Service of the National Oceanic and Atmospheric Administration, *J. Geophys. Res.*, *102*, 16,923–16,934, 1997.

Swap, R., M. Garstang, S. A. Macko, P. D. Tyson, W. Maenhaut, P. Artaxo, P. Kållberg, and R. Talbot, The long-range transport of southern African aerosols to the tropical South Atlantic, *J. Geophys. Res.*, *101*, 23,777–23,791, 1996.

Swap, R. J., H. J. Annegarn, and L. Otter, Southern African Regional Science Initiative (Safari 2000) summary of science plan, *S. Afr. J. Sci.*, *98*, 119–124, 2002.

Tanré, D., Y. J. Kaufman, M. Herman, and S. Mattoo, Remote sensing of aerosol properties over oceans using the MODIS/EOS spectral radiances, *J. Geophys. Res.*, *102*, 16,971–16,988, 1997.

Tanré, D., L. A. Remer, Y. J. Kaufman, S. Mattoo, P. V. Hobbs, J. M. Livingston, P. B. Russell, and A. Smirnov, Retrieval of aerosol optical thickness and size distribution over ocean from the MODIS Airborne Simulator during TARFOX, *J. Geophys. Res.*, *104*, 2261–2278, 1999.

Thompson, A. M., K. E. Pickering, D. P. McNamara, M. R. Schoeberl, R. D. Hudson, J. H. Kim, E. V. Browell, V. W. J. H. Kirchhoff, and D. Nganga, Where did ozone over southern Africa and the tropical Atlantic come from in October 1992? Insights from TOMS, GTE TRACE A, and SAFARI 1992, *J. Geophys. Res.*, *101*, 24,251–24,278, 1996.

Torres, O., P. K. Bhartia, J. R. Herman, A. Sinyuk, P. Ginoux, and B. Holben, A long-term record of aerosol optical depth from TOMS observations and comparison to AERONET measurements, *J. Atmos. Sci.*, *59*, 398–413, 2002.

Zhao, T. X.-P., L. L. Stowe, A. Smirnov, D. Crosby, J. Sapper, and C. R. McClain, Development of a global validation package for satellite oceanic aerosol optical thickness retrieval based on AERONET observations and its application to NOAA/NESDIS operational aerosol retrievals, *J. Atmos. Sci.*, *59*, 294–312, 2002.

D. A. Chu, C. Ichoku, Y. J. Kaufman, R. Levy, and L. A. Remer, Science Systems and Applications, Inc., NASA/GSFC code 913, Greenbelt, MD 20771, USA. (achu@climate.gsfc.nasa.gov; ichoku@climate.gsfc.nasa.gov; yoram.j.kaufman@nasa.gov; levy@climate.gsfc.nasa.gov; Lorraine.A.Remer@nasa.gov)

B. N. Holben, Laboratory for Terrestrial Physics, NASA/GSFC code 923, Greenbelt, MD 20771, USA. (Brent.N.Holben@nasa.gov)

D. Tanré, Laboratoire d'Optique Atmosphérique, Bat. P5, Université des Sciences et Technologies de Lille, F-59655 Villeneuve d'Ascq, France. (Didier.Tanre@univ-lille1.fr)